Title
Aberrant Striatal Activity in Parkinsonism and Levodopa-Induced Dyskinesia

Journal
Cell Reports, 23(12)

ISSN
2639-1856

Authors
Ryan, Michael B
Bair-Marshall, Chloe
Nelson, Alexandra B

Publication Date
2018-06-01

DOI
10.1016/j.celrep.2018.05.059

Peer reviewed

HHS Public Access

Author manuscript

Cell Rep. Author manuscript; available in PMC 2019 March 08.

Published in final edited form as:

Cell Rep. 2018 June 19; 23(12): 3438–3446.e5. doi:10.1016/j.celrep.2018.05.059.

Aberrant Striatal Activity in Parkinsonism and Levodopa-Induced Dyskinesia

Michael B. Ryan[1,2,3], **Chloe Bair-Marshall**[4], and **Alexandra B. Nelson**[1,2,3,4,5,*]

[1]Neuroscience Graduate Program, UCSF, San Francisco, CA 94158, USA

[2]Weill Institute for Neurosciences, UCSF, San Francisco, CA 94158, USA

[3]Kavli Institute for Fundamental Neuroscience, UCSF, San Francisco, CA 94158, USA

[4]Department of Neurology, UCSF, San Francisco, CA 94158, USA

[5]Lead Contact

Summary

Action selection relies on coordinated activity of striatal direct and indirect pathway medium spiny neurons (dMSNs and iMSNs, respectively). Loss of dopamine in Parkinson's Disease is thought to disrupt this balance. While dopamine replacement with levodopa may restore normal function, the development of involuntary movements (levodopa-induced dyskinesia, LID) limits therapy. How chronic dopamine loss and replacement with levodopa modulate firing of identified MSNs in behaving animals is currently unknown. Using optogenetically labeled striatal single-unit recordings, we assess circuit dysfunction in parkinsonism and LID. Counter to current models, we found that following dopamine depletion, iMSN firing was elevated only during periods of immobility, while dMSN firing was dramatically and persistently reduced. Most notably, we identified a subpopulation of dMSNs with abnormally high levodopa-evoked firing rates, which correlated specifically with dyskinesia. These findings provide key insights into the circuit mechanisms underlying parkinsonism and LID, with implications for developing novel, targeted therapies.

Introduction

In Parkinson's Disease (PD), progressive degeneration of midbrain dopamine neurons is associated with marked motor impairments, including bradykinesia (slowed movement), tremor, and rigidity. While the precise effect of dopamine loss on cellular and circuit function is unknown, dopamine replacement therapy with levodopa is the mainstay treatment. Levodopa is initially effective in treating PD motor deficits, but with chronic treatment the majority of patients develop drug-induced involuntary movements (Ahlskog

*Correspondence: alexandra.nelson@ucsf.edu.

Author Contributions

MBR and ABN designed the experiments. MBR conducted the electrophysiological recordings and analysis. MBR, ABN, and CBM conducted optogenetic stimulation experiments. MBR and ABN wrote the manuscript.

Declaration of Interests

The authors declare no competing interests.

and Muenter, 2001), known as levodopa-induced dyskinesia (LID). This clinical problem highlights the importance of identifying the circuit dysfunction resulting from dopamine loss and subsequent replacement with levodopa.

Midbrain dopamine neurons send their densest projections to the input nucleus of the basal ganglia, the striatum (Haber et al., 2000). Integrating dopaminergic inputs and glutamatergic inputs from sensorimotor cortical regions (McGeorge and Faull, 1987), the striatum is poised to control movement and decision-making (Redgrave et al., 2010). Dopamine is hypothesized to regulate movement via antagonistic control of GABAergic striatal projection neurons: direct and indirect pathway medium spiny neurons (MSNs). Direct pathway neurons (dMSNs) express the D_1-like dopamine receptor (Gerfen et al., 1990) and optical activation of dMSNs inhibits basal ganglia output and increases movement (Kravitz et al., 2010). Indirect pathway neurons (iMSNs) express the D_2-like dopamine receptor (Gerfen et al., 1990) and optical activation of iMSNs increases basal ganglia output and suppresses movement (Kravitz et al., 2010). According to the standard model of basal ganglia function, striatal dopamine release excites dMSNs and inhibits iMSNs, leading to action selection (Albin et al., 1989; DeLong, 1990). While pharmacological studies in *ex vivo* brain slices support this hypothesis (Hernández-López et al., 2000; Hernández-López et al., 1997; Planert et al., 2013), it is less clear how dopamine modulates striatal activity *in vivo*.

The standard model also predicts that dopamine loss, as occurs in PD, causes opposing changes in the activity of MSNs: persistently reduced dMSN and increased iMSN firing rates. Indirect support for this model derives from recordings in downstream basal ganglia nuclei in patients and parkinsonian primates (Bergman et al., 1994; Filion and Tremblay, 1991; Soares et al., 2004). However, direct evidence for bidirectional regulation of striatal MSN firing by dopamine in awake, behaving parkinsonian animals is lacking. As a corollary of this model, dopamine replacement with levodopa is postulated to improve motor symptoms by rebalancing striatal dMSN and iMSN activity. In addition, the prevailing hypothesis is that long-term levodopa treatment causes excessive direct pathway activity (Albin et al., 1989; DeLong, 1990), which may lead to LID. Again, some indirect evidence supports this model: altered firing in the striatum (Liang et al., 2008) and downstream basal ganglia nuclei (Boraud et al., 1998; Levy et al., 2001; Lozano et al., 2000; Papa et al., 1999), as well as pathway-specific changes in striatal gene expression in patients and animals models of LID (Heiman et al., 2014; Jenner, 2008). Crucially, once LID develops, a given dose of levodopa relieves parkinsonism *and* produces dyskinesia, suggesting that distinct mechanisms may mediate these levodopa-evoked behaviors. If these behavioral effects were indeed mediated by discrete cell types, targeted therapies could be more effective than levodopa alone.

Results

To determine how dopamine depletion and replacement with levodopa affect striatal activity, we performed optogenetically labeled single-unit recordings in the dorsolateral striatum (DLS) of freely moving parkinsonian mice (Figures 1A-1D). To render mice parkinsonian, we injected the neurotoxin 6-hydroxydopamine (6-OHDA) in the left medial forebrain

bundle (Figure S1A), causing a nearly complete depletion of ipsilateral dopamine (Figure S1B). As a result, parkinsonian mice showed reduced movement velocity and predominantly ipsilesional rotations. After six weeks, mice began daily levodopa injections in conjunction with recording sessions. A typical recording session consisted of a baseline (parkinsonian) period, followed by levodopa injection (5 mg/kg; Figure S1D), which caused both dyskinesia (LID; Figures 1E and S1C) and contralesional rotations (Figure 1F). Optogenetic labeling of dMSNs and iMSNs was achieved by expressing channelrhodopsin-2 (ChR2; Figure S1B) selectively in dMSNs or iMSNs (using D1-Cre or A2a-Cre mice, respectively) (Gerfen et al., 2013; Gong et al., 2007), and recording responses to light pulses at the end of each session. Following established protocols (Kravitz et al., 2013), we identified optogenetically labeled neurons as those with short latency light-evoked firing (Figure 1D).

Dopamine Depletion Reduces the Firing Rate of dMSNs

The standard model predicts that dopamine loss causes persistent decreases in dMSN and increases in iMSN firing. To determine whether chronic dopamine depletion causes opposing changes in MSN activity, we compared the firing rate of optogenetically labeled dMSNs and iMSNs in parkinsonian mice to those in healthy mice. As predicted, labeled dMSNs from parkinsonian mice fired at dramatically lower rates than in controls (Park: 0.11 ± 0.04 Hz, n=14, N=10; Ctrl: 1.61 ± 0.19 Hz, n=64, N=5, $p<0.0001$, Mann-Whitney; Figures 1G and S1E). Surprisingly, the average firing rate of iMSNs was not significantly increased in parkinsonian mice (Park: 1.24 ± 0.23 Hz, n=32, N=8; Ctrl: 1.42 ± 0.28 Hz, n=34, N=5, $p=0.852$, Mann-Whitney; Figures 1H, middle and S1F). This imbalance in dMSN and iMSN activity was also specific to the depleted hemisphere. While activity in the contralesional striatum was lower compared to healthy controls (Contra: 0.78 ± 0.14 Hz, n=88, N=5, $p<0.0001$, Mann-Whitney), as previously reported (Chen et al., 2001; Kish et al., 1999; Oye et al., 1970), we found that dMSNs (0.84 ± 0.23 Hz, n=5, N=2) and iMSNs (0.73 ± 0.18, n=5, N=2) had similar rates ($p=0.99$, Mann-Whitney, not shown). These results demonstrate that dopamine loss produces a marked and persistent reduction in ipsilesional dMSN firing, resulting in an imbalance between dMSN and iMSN activity.

Levodopa Causes Bidirectional Dysregulation of MSN Firing Rates During LID

By increasing striatal dopamine, levodopa is hypothesized to restore the normal balance of striatal activity via bidirectional modulation of dMSNs and iMSNs. In LID, amplification of this modulation may trigger involuntary movements. To test whether levodopa increases dMSN and decreases iMSN firing rates, we recorded optogenetically identified MSNs before and after levodopa administration in parkinsonian mice. As predicted by the standard model, levodopa increased dMSN firing rates (3.44 ± 0.93 Hz, n=9, N=6, $p=0.004$, Wilcoxon; Figures 1G and S1E) and decreased iMSN firing rates (0.38 ± 0.22 Hz, n=16, N=6, $p<0.0001$ Wilcoxon; Figures 1H and S1F). Furthermore, during LID, the average firing rate of dMSNs was more than double the rate in healthy controls ($p=0.035$, Mann-Whitney; Figures 1G, middle and S1E). Levodopa also decreased the firing rate of iMSNs below rates in healthy mice ($p<0.0001$, Mann-Whitney; Figures 1H, middle and S1F). These findings confirm that MSNs are in fact bidirectionally modulated by levodopa, and further, that LID is associated with firing rates outside the normal range for both dMSNs and iMSNs.

We also found that the directionality of neural responses was extremely consistent: no dMSN was inhibited and no iMSN was excited by levodopa. Using this reliable response of optogenetically labeled MSNs, we classified unlabeled MSNs based on levodopa-evoked firing rate change. Units with a significant levodopa-evoked increase or decrease in firing rate were classified as putative dMSNs (On, n=146, N=15) or iMSNs (Off, n=69, N=15), respectively (Figure S1G, left and middle). Units with no significant change could not be classified (No Change, n=40, N=15; Figure S1G, right). In this larger pool, we found that putative MSNs showed similar firing rates to their optogenetically labeled counterparts (Figures S1H-S1K), providing further evidence that striatal activity is dysregulated in parkinsonism and LID.

Dopamine Receptor Specific Agonists Mimic the Effects of Levodopa

While these results point toward bidirectional dysregulation of dMSNs and iMSNs as an underlying feature of LID, levodopa-evoked dopamine release might directly *or* indirectly influence dMSN and iMSN firing through activation of D_1-like (D1R) and D_2-like (D2R) dopamine receptors located on several microcircuit elements (Gerfen and Surmeier, 2011). We sought to assess how selective activation of D1R or D2R compared to combined activation with levodopa. Remarkably, we found that administration of the selective D1R agonist SKF-81297 (SKF) also produced bidirectional regulation of striatal neurons, much like levodopa (On MSN: 0.10 ± 0.05 Hz (Park) vs 2.20 ± 0.39 Hz (SKF), n=23, N=5, $p<0.0001$, Wilcoxon; Off MSN: 0.93 ± 0.33 Hz (Park) vs 0.19 ± 0.08 Hz (SKF), n=9, N=5, $p=0.004$, Wilcoxon), while evoking robust dyskinesia and contralesional rotations (Figures S2A-S2E). Administration of the selective D2R agonist Quinpirole (Quin) also produced bidirectional regulation of striatal neurons, albeit with more modest firing rate changes in activated neurons (On MSN: 0.18 ± 0.05 Hz (Park) vs 0.76 ± 0.10 Hz (Quin), n=19, N=6, $p<0.0001$, Wilcoxon; Off MSN: 1.22 ± 0.39 Hz (Park) vs 0.18 ± 0.05 Hz (Quin), n=12, N=6, $p<0.0001$, Wilcoxon), while evoking contralesional rotations and more modest dyskinesia (Figures S2F-S2J). Interestingly, each of these agonists modulated a similar proportion of striatal neurons compared to levodopa (Figure S2K), highlighting the effects of dopamine receptor activation on striatal microcircuitry through both direct regulation of MSNs *and* indirect modulation of synaptic (local inhibitory and/or excitatory extra-striatal) inputs.

Locomotor Modulation of dMSN and iMSN Firing Is Impaired in Parkinsonism and LID

As movement robustly modulates striatal activity (Barbera et al., 2016; Cui et al., 2013; Jin et al., 2014), we next sought to determine how locomotion affected the firing rate of MSNs in control and parkinsonian mice. In healthy controls, we found a positive correlation between velocity and firing rate for both dMSNs and iMSNs (Figures S1L-S1N, bottom). We quantified this locomotor modulation by averaging the firing rate of MSNs during mobile (velocity > 3 cm/s) and immobile (velocity < 0.5 cm/s) epochs. As expected, we observed higher firing rates during locomotion for both dMSNs and iMSNs in healthy controls (dMSNs (n=41, N=5), iMSNs (n=25, N=5), and all MSNs (n=67, N=10), $p<0.0001$, Wilcoxon; Figures S1L-S1N, top). MSNs recorded in the contralesional striatum of parkinsonian mice also retained this modulation, with higher firing rates during locomotion (n=88, N=5, $p<0.0001$, Wilcoxon; Figure S1L). However, in the ipsilesional striatum the firing rate of dMSNs was not modulated by locomotion (n=144, N=12, $p=0.624$, Wilcoxon),

and iMSN firing rates were *lower* during locomotion (n=68, N=12, p=0.005, Wilcoxon; Figures S1M-S1N). Interestingly, though overall iMSN firing rates in parkinsonian mice were not significantly different than in healthy controls (Figure 1H), iMSN firing rates were significantly higher specifically during epochs of immobility (Park: 1.71 ± 0.21 Hz vs Ctrl: 0.69 ± 0.15 Hz, p<0.0001, Mann-Whitney), but not locomotion (Park: 1.37 ± 0.23 Hz vs Ctrl: 1.55 ± 0.28 Hz, p=0.313, Mann-Whitney, Figure S1N). Levodopa administration caused robust changes in overall firing rate (Figure 1), but did not restore locomotor modulation: dMSNs showed no significant modulation (p=0.181, Wilcoxon) and iMSNs showed lower firing during locomotion (p<0.0001, Wilcoxon; Figures S1L-S1N). These data indicate that dopamine depletion persistently decreases dMSN firing, increases iMSN firing specifically during immobility, and further, that both dMSNs and iMSNs show reduced locomotor modulation, which is not restored by levodopa.

Activation of dMSNs Is Sufficient to Cause Dyskinesia, Which Is Potentiated by Chronic Levodopa Treatment

While the preceding experiments demonstrate that dMSNs exhibit high firing rates during LID, they do not prove whether dMSN activity is *sufficient* to cause dyskinesia. Using optogenetic stimulation of dMSNs in the DLS of healthy and parkinsonian mice, we tested whether dMSN activation causes dyskinesia (Figures 2A–2B). In parkinsonian D1-Cre mice injected with ChR2, we calibrated laser power to evoke firing rates similar to those seen during LID. Blue light at 1 mW elicited dMSN firing rates (3.98 ± 1.37 Hz, n=9, N=7) comparable to those seen in dMSNs during LID (4.61 ± 1.23 Hz; Figure 1G). Stimulation produced both dyskinesia and contralateral rotations, in the absence of levodopa (Figures 1D-1E and Movie S1). Light-evoked dyskinesia was time-locked to light and increased in severity at higher powers (Figures S3A-S3B). Interestingly, we observed similar dyskinesia and contralateral rotations when stimulating the non-depleted hemisphere (Figures S3C-S3D). Bilateral stimulation also produced dyskinesia and increased movement velocity (Figures S3E-S3F). These results suggest that dopamine depletion may not be necessary for dMSN-mediated dyskinesia.

Indeed, it is widely debated how progressive dopamine depletion and chronic levodopa treatment independently influence the development of LID (Ahlskog and Muenter, 2001; Horstink et al., 1990). Dyskinesia is observed in advanced PD patients chronically treated with levodopa, making it difficult to disentangle their individual contributions. To determine how dopamine depletion and chronic levodopa treatment modulate dMSN-mediated movements, we compared the severity of dyskinesia and number of contralateral rotations with dMSN stimulation between three groups: levodopa-naïve and chronically levodopa-treated parkinsonian mice, and healthy mice. First, to look at whether dopamine depletion itself increased severity of dMSN-mediated dyskinesia, we compared parkinsonian and healthy mice, and found no significant difference in dyskinesia during optical stimulation (Park (N=8) vs Ctrl (N=12), p=0.881, Mann-Whitney; Figures 2D-2E, top). Second, to determine how chronic levodopa treatment altered dMSN-mediated dyskinesia, we compared parkinsonian mice (N=8) before (levodopa-naïve) and after chronic levodopa treatment to healthy mice (N=12). Chronically treated mice showed significantly more optically-evoked dyskinesia than both levodopa-naïve parkinsonian (p=0.001, Wilcoxon)

and healthy (p=0.014, Mann-Whitney) mice (Figures 2D-2F, top). Contralateral rotations were not significantly different between groups (Figures 2D-2F, bottom), suggesting that levodopa exposure may enhance vulnerability to dyskinesia, as opposed to other motor effects. Together, these findings support the idea that chronic levodopa treatment, perhaps more than dopamine loss itself, primes basal ganglia circuitry for dMSN-mediated dyskinesia.

A Subpopulation of dMSNs Exhibit High Firing Rates Correlated to Dyskinesia

One prominent hypothesis in the field posits that over-activation of dMSNs underlies LID. Indeed, we observed heterogeneity in dMSN responses to levodopa, with only a subset of dMSNs exhibiting high firing rates (Figure 1G). To identify dMSNs with abnormally high levodopa-evoked firing rates, we compared the rates of putative dMSNs from parkinsonian mice to labeled MSNs from healthy mice. Putative dMSNs with levodopa-evoked firing rates within the 99% confidence interval of MSN firing rates from healthy mice were classified as Moderate FR (58%), while those exceeding this threshold were classified as High FR units (42%; Figure S4A). Moderate and High FR units were commonly observed on nearby electrodes and in the same session (Figures 3B and 3D). Moreover, High FR units were rarely observed in the subset of sessions in which levodopa did not elicit dyskinesia (3%, n=30, N=4). These results indicate dMSNs have a heterogeneous response to levodopa, with only a subset of dMSNs showing excessive activity.

If high firing dMSNs are causally involved in dyskinesia, their firing may be closely correlated to the severity or onset of dyskinesia. We tested this hypothesis by calculating the correlation between individual unit firing rates and dyskinesia, as well as levodopa-evoked rotations. Some dMSNs displayed strong correlations to dyskinesia but minimal correlation to rotations (DYSK, n=47, N=15; Figures 3A-3B), while others correlated to rotational behavior, and not dyskinesia (ROT, n=14, N=15; Figures 3C-3E). Other cells did not show a strong correlation to either behavior (ON, n=74, N=15; Figures 3E-3F). Remarkably, the activity of most High FR units correlated with dyskinesia (Figures 3B and 3G), while the activity of Moderate FR units rarely correlated with dyskinesia (Figures 3D, 3F, 3G and Movie S2). Conversely, we categorized units by their behavioral correlation and examined their parkinsonian and levodopa-evoked firing rates. We found that all dMSN subpopulations showed similar firing rates following dopamine loss, which were all significantly lower than healthy controls (One-Way ANOVA $F(3,229)=27.33$, $p<0.0001$, Tukey post-hoc, Ctrl vs Park: $p<0.01$; Figure 3H). Interestingly, levodopa-evoked ON and ROT unit firing rates were not significantly different than those seen in healthy mice, while DYSK unit firing rates were significantly higher (One-Way ANOVA $F(3,229)=43.63$, $p<0.0001$, Tukey post-hoc, Ctrl vs LID: ON ($p>0.05$), ROT ($p>0.05$), and DYSK ($p<0.01$); Figure 3H). Additionally, we compared the relative onset of firing rate changes and dyskinesia in these dMSN subpopulations. We found that average DYSK unit firing significantly increased 31.6 ± 13.2 seconds prior to the onset and decreased 38.1 ± 18.4 seconds prior to end of LID (Figure 3I), with most DYSK units showing a firing change before the start (72%) and end (65%) of dyskinesia. In contrast, the firing rate of ROT and ON units showed no clear relationship to the start or end of dyskinesia (Figures S4B-S4C). Therefore, as their firing tends to precede

dyskinesia onset and correlate with dyskinesia severity on a fine timescale, DYSK units are poised to influence the development of dyskinesia.

To determine if DYSK unit firing was *specific* to LID, we injected mice with two doses of levodopa in a single session: a moderate (dyskinetic) dose and a lower (sub-dyskinetic) dose of levodopa, which produced contralesional rotations, but no dyskinesia. We found that ROT and ON units were activated by levodopa in the absence of dyskinesia, showing a graded response to levodopa dosage (Figures 4A and 4C). Interestingly, we found that DYSK units were not modulated by lower (sub-dyskinetic) doses of levodopa (Park: 0.07 ± 0.05 Hz vs sub-dyskinetic: 0.35 ± 0.16 Hz, n=8, N=3, p=0.078, Wilcoxon), but robustly activated at moderate (dyskinetic) doses (LID: 5.03 ± 2.1 Hz, p=0.008, Wilcoxon; Figures 4B-4C and Movie S3). In addition, DYSK units showed little to no modulation during grooming, a qualitatively similar behavior which involves many of the same body regions (0.24 ± 0.14 Hz vs LID: 6.27 ± 0.67 Hz, n=44, N=5, p<0.0001, Wilcoxon), while a subset of ON units was modulated by grooming (Figure 4D and Movie S4). In fact, as compared to ON units (n=30, N=4), DYSK units showed much lower firing rates during grooming (ON: 0.99 ± 0.34 Hz vs DYSK 0.24 ± 0.14 Hz, p=0.003, Mann-Whitney, Figure 4D), suggesting their firing properties are not solely the result of sensorimotor feedback. Together, these results demonstrate that DYSK unit firing is specific to the dyskinetic state, suggesting these dMSNs represent a distinct and stable subpopulation in parkinsonian animals.

Discussion

Here, we directly tested fundamental tenets of the standard model: (1) loss of dopamine reduces dMSN and increases iMSN firing rates, (2) levodopa bidirectionally modulates dMSNs and iMSNs, and (3) LID is associated with excessive dMSN activity. Using optogenetically labeled single-unit recordings in parkinsonian mice, we found that dopamine depletion markedly and persistently reduced dMSN firing rates compared to healthy controls, while iMSN firing was elevated only during periods of immobility. Levodopa evoked bidirectional modulation of MSNs beyond firing rates normally observed, with dramatically elevated levodopa-evoked firing rates in a subset of dMSNs. Consistent with a dMSN-mediated mechanism of LID, optogenetic stimulation of dMSNs was sufficient to trigger dyskinesia in healthy and parkinsonian mice, and was potentiated following chronic levodopa treatment. Finally, we found functional subdivisions within the direct pathway: levodopa elicited high firing rates in a subset of dMSNs, whose firing rates strongly correlated with dyskinesia severity, suggesting a subpopulation of dMSNs which may be causally involved in LID.

Though many investigators have posited that loss of dopaminergic input results in persistent elevation of iMSN firing, we observed elevated iMSN activity only when the animal was immobile. Most evidence for increased iMSN activity in parkinsonism is indirect, based on downstream basal ganglia nuclei (Bergman et al., 1994; Filion and Tremblay, 1991; Galvan et al., 2015; Soares et al., 2004) in restrained nonhuman primates. These nuclei, however, integrate striatal *and* extrastriatal inputs; the latter perhaps more important for shaping output (Deffains et al., 2016). In anesthetized parkinsonian rodents, one recent study of identified iMSNs found no change in firing rate (Ketzef et al., 2017), while an older study of

putative iMSNs showed a very modest increase (0.5 spikes/s) in the firing rate (Mallet et al., 2006). Intrinsic excitability and synaptic inputs may drive MSN firing differently under anesthesia than in an awake, behaving animal, accounting for these differences. Another study employing acute dopamine depletion in awake mice found increased firing in a subset of unidentified striatal neurons (Costa et al., 2006). While transient reduction of striatal dopamine might increase iMSN activity, changes following chronic dopamine loss, such as reduced intrinsic excitability (Fieblinger et al., 2014), may compensate for the loss of D_2-like receptor mediated inhibition. In support of the standard model, levodopa evoked pronounced bidirectional changes in striatal activity. Studies in ex vivo brain slices showing opposing changes in striatal intrinsic excitability and corticostriatal synaptic plasticity offer potential mechanisms for these findings (Fieblinger et al., 2014; Picconi et al., 2003; Shen et al., 2015). Notably, we found similar bidirectional changes in MSN firing using a selective D1R or D2R agonist in place of levodopa. As there are no D1Rs on iMSNs, nor D2Rs on dMSNs, this observation implies dopaminergic agents produce convergent changes in striatal firing through both intrinsic and synaptic mechanisms. In fact, a recent study combining a selective D2R agonist and chemogenetic manipulations of dMSNs highlights the interactions between the two pathways in modulating dyskinesia (Alcacer et al., 2017). Taken together, these results suggest that while elevated iMSN firing is not a static feature of parkinsonism, inhibition of iMSNs may still contribute to levodopa-evoked facilitation of movement.

By optogenetically activating dMSNs in the DLS of healthy and parkinsonian mice, we evoked dyskinesia in the absence of levodopa, which was potentiated following chronic levodopa treatment. These findings are in line with recent reports of manipulating dMSNs optically (Perez et al., 2017; Rothwell et al., 2015) and chemogenetically (Alcacer et al., 2017) to evoke dyskinesia in mice. Notably, stimulation of dMSNs in the dorsomedial striatum (in contrast to the DLS) relieves parkinsonism without inducing dyskinesia (Kravitz et al., 2010). This difference underscores the functional heterogeneity of dMSNs within dorsal striatum; thus highlighting the DLS as a candidate locus for dyskinesia, as suggested by pharmacological studies (Carta et al., 2006; Yoshida, 1991). Given the increased intrinsic excitability observed in brain slices from parkinsonian mice (Fieblinger et al., 2014), we expected an increase in optically evoked dyskinesia compared to healthy controls. However, homeostatic mechanisms in striatal synaptic transmission or intrinsic excitability of downstream basal ganglia nuclei may compensate for enhanced dMSN excitability.

Our recordings of dMSNs within the DLS also showed heterogeneity in levodopa responses, which has been suggested by recordings of unidentified striatal neurons in parkinsonian primates (Liang et al., 2008). We found that levodopa evoked normal firing rates in some dMSNs and elevated rates in others. The firing rate of these latter neurons also strongly correlated with dyskinesia severity on a fine timescale and was specific for dyskinesia compared to other levodopa-evoked and spontaneous behaviors (ie. grooming). Levodopa produces both relief of parkinsonism *and* dyskinesia. Our results suggest a possible mechanism: restoration of normal firing rates in a subset of dMSNs may mediate therapeutic effects, and excessive firing in another subset may mediate dyskinesia. While additional experiments will be necessary to firmly establish causal relationships between dMSN subtypes and dyskinesia, these findings highlight the functional diversity of dMSNs in LID.

If these MSN subtypes represent distinct cell populations, by virtue of molecular markers or connectivity, they offer a potential therapeutic target in LID.

Star Methods

Contact for Reagent and Resource Sharing

Further information and requests for resources and reagents should be directed to and will be fulfilled by the Lead Contact, Alexandra Nelson (Alexandra.Nelson@ucsf.edu).

Experimental Model and Subject Details

Animals—Hemizygous BAC transgenic mice expressing Cre recombinase under the control of the Drd1a (D1-Cre, GENSAT BAC transgenic EY217) or Adora2a (A2a-Cre, GENSAT BAC transgenic KG139) regulatory elements were used to restrict expression of Cre-dependent constructs to direct and indirect pathway striatal neurons, respectively. All mice were on a C57Bl/6 background and housed under a 12-h light/dark cycle with food and water *ad libitum*. Male and female mice were used. All experiments were conducted with the approval of the Institutional Animal Care and Use Committee at the University of California, San Francisco and complied with local and national ethical and legal regulations regarding the use of mice in research.

Method Details

Unilateral 6-OHDA Model—Six- to ten-week-old mice were anesthetized with a combination of intraperitoneal (i.p.) ketamine/xylazine (40/10 mg/kg) for induction and inhaled isoflurane (1%) for maintenance of anesthesia. In the stereotaxic frame (Kopf Instruments), the scalp was opened and a hole drilled through the skull over the medial forebrain bundle (MFB). After puncturing the dura, 1 μL of 6-hydroxydopamine (6-OHDA; Sigma-Aldrich, 5 μg/μL in normal saline) was injected unilaterally into the left MFB at the following coordinates relative to bregma and cortical surface: AP −1.0, ML −1.0, DV −4.9, through a 33 gauge cannula (Plastics One) and syringe pump (Harvard Apparatus). To minimize uptake of the toxin by noradrenergic and serotonergic axons, desipramine (Sigman-Aldrich, 25 mg/kg i.p.) was administered immediately prior to surgery. Post-operatively, mice were monitored daily and supplemented with saline injections and high-fat diet as needed (Francardo et al., 2011). Ipsilesional rotations were quantified in open-field using video tracking (Noldus Ethovision) periodically over two weeks to verify dopaminergic lesion and hemiparkinsonism.

Virus Injections and Implants—DIO constructs were used to express ChR2-eYFP or eYFP alone specifically in Cre-positive cells. For *in vivo* electrophysiology experiments, 6-OHDA-treated D1-Cre and A2a-Cre mice were anesthetized, the scalp reopened, and a large craniectomy (1.5 × 1 mm) made over the left dorsolateral striatum (DLS). 1.5 μL of AAV5-EF1a-DIO-hChR2(H134R)-eYFP-wpre-hGH (UPenn Vector Core, 1:1 dilution in normal saline) was injected into the ipsilesional DLS (AP +0.8, ML −2.3, DV −2.5 from cortical surface), using a 33 gauge cannula and syringe pump. Three additional holes were drilled for two skull screws (FST) and a ground wire. A fixed multichannel optrode (32-channel microwire (35 μm tungsten) array (Innovative Neurophysiology) coupled to a 200 μm optical

fiber (Thorlabs)) was slowly inserted through the craniectomy into the DLS to a final depth 100-200 μm above the viral injection. A thin layer of dental cement (Metabond, Parkell) was applied to the surface of the skull and dental acrylic (Ortho-Jet, Lang Dental) was applied to cover all exposed hardware. The same procedures were followed for *in vivo* electrophysiology experiments in the right (contralesional) DLS (AP +0.8, ML +2.3, DV −2.5 from cortical surface) of 6-OHDA-treated D1-Cre and A2a-Cre mice.

For direct pathway stimulation experiments, D1-Cre mice were anesthetized, the scalp exposed, and small holes drilled bilaterally above the DLS. 1 μL of DIO-ChR2-eYFP virus (1:1 dilution as above) or AAV5-EF1a-DIO-eYFP (UNC Vector Core) was injected bilaterally into the DLS (AP +0.8, ML ±2.3, DV −2.5 from cortical surface) of healthy or 6-OHDA treated mice (4-6 weeks after 6-OHDA injection). Optic fiber-ferrule assemblies (200 μm, Thorlabs) were implanted bilaterally 100-200 μm above each viral injection. Dental cement was applied to the scalp and the base of exposed ferrules was covered with dental acrylic. To allow for adequate expression, mice were housed for at least two weeks following viral injections before any electrophysiology or behavioral experiments began.

Behavior—Animals were acclimated to the open field (25 cm diameter acrylic cylinder, Tap Plastics) for 1-2 sessions prior to experiments. Gross movement (velocity, rotations) was measured using a top-mounted video camera and video tracking software (Noldus Ethovision). Ipsilesional and contralesional rotations were identified using a Noldus Ethovision analysis module, with a rotation threshold of 90° and a minimum distance traveled of 2 cm. Dyskinesia was quantified using the Abnormal Involuntary Movement score (AIMs), an established method of scoring levodopa-induced dyskinesia (Cenci and Lundblad, 2007). The start and end of dyskinesia were scored in 2 second bins and defined as the first and last observable dyskinetic movement (of any body segment), respectively. For optical stimulation experiments (described below in the Optogenetic Stimulation section), two mice were run at a time, gross movement measured using video tracking, and dyskinesia manually scored by raters blinded to the viral injection.

Pharmacology—Levodopa (Sigma Aldrich), in combination with benserazide (Sigma Aldrich), was dissolved in normal saline and administered daily (5 days per week) by i.p. injection. A dose of 2.5-5.0 mg/kg of levodopa (plus 1.25-2.5 mg/kg benzeraside) typically elicited dyskinetic movements and contralesional rotations. Lower doses of levodopa (0.5-2.5 mg/kg) were administered in some sessions to elicit therapeutic behavioral responses (defined as increased contralateral rotations) without dyskinesia (sub-dyskinetic dose; Figure 4). The D1R-selective agonist SKF-81297 or the D2R-selective agonist Quinipriole (Tocris Bioscience) were administered in place of levodopa in interleaved sessions. SKF-81297 (3-5 mg/kg) and Quinpirole (0.5-2 mg/kg) were dissolved in normal saline and injected i.p., eliciting both dyskinesia and contralesional rotations (Figure S2).

***In Vivo* Electrophysiology—**During each recording session, the animal was placed in the open-field while tethered via a lightweight, multiplexed headstage cable (Triangle Biosystems) attached to a low-torque electrical commutator (Dragonfly) to allow free movement. The animal's gross behavior was recorded by video tracking software (Noldus Ethovision). Fine behavior was manually scored by the experimenter (AIM score).

Behavioral measurements were synchronized with simultaneous electrophysiological recordings via TTL pulses triggered by the video tracking software and recorded by the electrophysiology system (MAP system, Plexon). Animals were habituated to tethering and i.p. injections (saline) prior to pharmacological experiments.

In parkinsonian animals, a typical recording session consisted of a 30 minute baseline period during which animals displayed ipsilesional biased rotations, followed by i.p. injection of levodopa (Figure S1D). Contralesional rotations and levodopa-induced dyskinesia (LID) typically began within 10 minutes of injection, lasted between 30-120 minutes and terminated spontaneously. At the end of each session, once the animal had returned to baseline behavior, a fiber optic patch cable was connected to the animal's implant and the optogenetic labeling protocol commenced (see Optogenetic Labeling section below). Optogenetically labeled cells from healthy (control) mice were collected as part of another study, and a 30-minute baseline period from these recordings was used for comparison with parkinsonian recordings performed using the same techniques. Optogenetically labeled and unlabeled cells from the contralesional striatum of parkinsonian mice were also collected during an equivalent 30-minute baseline period in which animals displayed ipsilesional biased rotations, performed using the same techniques.

In a subset of recordings, parkinsonian mice were administered an additional i.p. injection of levodopa at a sub-dyskinetic dose during a single session (Figure 4). In these experiments, the first injection of levodopa (dyskinetic or sub-dyskinetic dose was randomly chosen) occurred after the 30-minute baseline period as described above. After the animal had returned to baseline parkinsonian behavior, the second injection of levodopa was administered. Once the behavior again returned to baseline, the optogenetic labeling protocol was initiated.

Signal acquisition—Single unit activity from microwires was recorded using a 32-channel recording system (MAP system, Plexon). Spike waveforms were filtered at 154-8800 Hz and digitized at 40 kHz. The experimenter manually set a threshold for storage of electrical events.

Spike Sorting and Cell Classification—Single units (SUs) were identified offline by manual sorting into clusters (Offline Sorter, Plexon). Waveform features used for separating units were typically a combination of valley amplitude, the first three principal components (PCs), and/or nonlinear energy. Clusters were classified as SUs if they fulfilled the following criteria: (1) <1% of spikes occurred within the refractory period and (2) the cluster was statistically different ($p<0.05$, MANOVA using the aforementioned features) from the multi- and other single-unit clusters on the same wire. SUs were then classified as putative medium spiny neurons (MSNs) as previously described (Berke et al., 2004; Gage et al., 2010; Harris et al., 2000) using features of the spike waveform (peak to valley and peak width), as well as inter-spike interval distribution. Only putative MSNs were included in subsequent analyses.

Optogenetic Labeling—TTL-controlled blue laser (493 nm; Shanghai Laser and Optics Century) pulses were delivered to the optrode array via a fiber optic patch cable (200 μm; Thorlabs) connected to an optical commutator (Doric Lenses). A series of brief light pulses

(1000 pulses, 150 sec duration, 1 Hz) were delivered at varying light intensities (0.5, 1, 2, and 4 mW light power at the tip of the fiber optic patch cable). Light intensity was measured daily with a light meter (Thorlabs) and calibrated for each light power. To determine if a putative MSN was optogenetically labeled, a peristimulus time histogram, aligned to laser onset, was constructed (Figure 1D). A SU was considered optogenetically labeled if it fulfilled the following criteria: (1) firing rate increased above the 95% confidence interval of pre-laser firing rate within 15 msec of laser onset, (2) firing rate remained above this threshold for at least 15 msec, and (3) laser-evoked waveforms were not different than spontaneous waveforms (correlation coefficient (R^2) > 0.9).

Optogenetic Stimulation—TTL-controlled blue laser light (473 nm; Shanghai Laser and Optics Century) was delivered to fiber-ferrule assembly via a fiber optic patch cable (200 μm; Thorlabs) connected to a dual-output optical commutator (Doric Lenses). Behavior (rotations and AIM score) was recorded over the course of a single session, which consisted of the following: a two minute baseline period with no laser illumination, then four trials of laser stimulation, followed by a two minute post-stimulation period (Figure 2C). Each trial consisted of a 30 sec laser on (constant illumination) and 30 sec laser off epoch (Figure 2C, Laser). Light intensity was measured daily and calibrated for 0.5, 1, 2, and 4 mW light powers at the tip of the fiber optic patch cable. Stimulation experiments were conducted at each of the above-mentioned light powers and were fixed for a given session. 6-OHDA treated mice received optogenetic stimulation both in the levodopa-naive state and again after chronic levodopa treatment (levodopa/benzeraside (10/5 mg/kg i.p.) daily for 2 weeks). Treatment was withheld on the day of optogenetic stimulation experiments.

Tissue Processing and Immunohistochemistry—Mice were terminally anesthetized with ketamine/xylazine (200/40 mg/kg i.p.), transcardially perfused with 4% paraformaldyde (PFA), and the brain dissected from the skull. The brain was post-fixed overnight in 4% PFA and then placed in 30% sucrose at 4°C. Using a freezing microtome (Leica), the brain was sliced into 30 μm coronal sections. In 6-OHDA treated mice, the extent of dopamine depletion was confirmed by TH immunohistochemistry, using standard protocols. Briefly, after washing sections in PBS (5 × 10 minutes) and blocking in normal donkey serum (NDS)/0.1% Triton-X (1 hour at room temperature, RT), we incubated sections in primary antibody (Pel-Freez rabbit anti-TH, 1:1000 at 4°C overnight). Adequate expression of viral DIO constructs (ChR2-YFP and YFP) was also verified. Briefly, sections were washed in PBS, incubated in fluorescently labeled secondary antibody (donkey anti-rabbit 647 nm, Jackson Immunoresearch; 1:500 in NDS at RT for 2 hours), and washed in PBS prior to mounting onto glass slides (Vectashield Mounting Medium). Sections were imaged in the YFP/GFP (excitation 488 nm, emission 509 nm) and Cy5 (excitation 650 nm, emission 684 nm) channels, verifying striatal ChR2-YFP or YFP-control expression and ipsilesional TH depletion. Only animals with >90% dopamine depletion were included in this study (Figure S1B). Stitched multi-channel fluorescence images were taken on a Nikon 6D conventional wide-field microscope at 4-10X, using custom software (UCSF Nikon Imaging Center). To verify the location of the optrode array in the DLS, under deep terminal anesthesia prior to transcardial perfusion, electrolytic lesions were made to mark electrode tips using a solid state, direct current Lesion Maker (Ugo Basile), by applying 100 μA for 5

sec per microwire. For optogenetic stimulation experiments, optic fiber placement in the DLS was verified by the location of tissue deformation made by the ferrule.

Quantification and Statistical Analysis

Behavior—Dyskinesia was quantified using the Abnormal Involuntary Movement score (AIMs) (Cenci and Lundblad, 2007). Briefly, abnormal axial, limb, and orolingual movements were scored manually by the experimenter for one minute every other minute for the total length of a dyskinetic episode (ranging from 30-120 minutes). The AIM scale ranges from 0 to 4 for each body segment, defined as follows for a given one minute observation period: a score of 0 represents normal movement, 1 represents abnormal movement for <50% of the time, 2 represents abnormal movement for >50% of the time, 3 represents abnormal movement for the entire period, but can be interrupted (for example, by tapping the chamber wall), and 4 represents uninterruptible, continuous abnormal movement. Total AIM score is the sum of AIM scores for the three body segments (axial, limb, orofacial; maximum score of 12).

Gross movement was quantified using several metrics. Rotation rate was calculated per minute by subtracting total ipsilesional from contralesional rotations. Locomotor activity was also quantified to identify discrete locomotor states, where we divided the behavioral session (using 2 second bins) into immobile (velocity < 0.5 cm/s) or mobile (velocity > 3 cm/s) epochs. For a more continuous measure, velocity was also quantified throughout the behavioral session (using 1 second bins). Grooming epochs were manually identified post-hoc from video of recorded behavioral sessions (using a 2 second minimum duration for classification).

***In Vivo* Electrophysiology—**For the majority of experiments, firing rate was averaged in 1 minute bins. Modulation of firing rate by levodopa (or dopamine agonists) was determined by comparing single unit (SU) firing rates before and after drug administration, during the peak behavioral effects. The 30-minute baseline period was compared to a 30-minute period following drug injection (10-40 minutes post-injection). Following levodopa administration, unlabeled SUs were categorized into three broad groups as follows, based on significant changes in firing rate ($p<0.01$, Wilcoxon rank-sum test (denoted Mann-Whitney)) following levodopa treatment: putative dMSNs (increase in firing rate), putative iMSNs (decrease in firing rate), or no change units (nonsignificant change in firing rate). Following agonist administration, the same analysis was used to identify SUs with significant increases (On MSNs), decreases (Off MSNs), or no change in firing rate (NC). For levodopa sessions, putative dMSNs were further divided using rate-based and behavior-based methods.

For the rate-based method, we compared SU firing rates of putative dMSNs from parkinsonian mice after levodopa injection to the firing rates of healthy mice. We calculated the 99% confidence interval of firing rate for all SUs recorded in healthy mice and used the upper bound of this interval as our threshold. A putative dMSN was classified as High FR if the post-levodopa firing rate (10-40 minutes post-injection of levodopa) exceeded the 99% confidence interval of MSNs from healthy mice in any single bin. A putative dMSN with a post-levodopa firing rate within the 99% confidence interval of healthy mice was classified

as a Mod FR unit (Figure 3G). For the behavior-based method, rotation rate and AIM score were also averaged in 1 minute bins and correlated with firing rate using linear regression. Putative dMSNs with a significant correlation (R^2>0.4) to rotation rate were labeled rotation (ROT) units, those with a significant correlation to AIM score were labeled dyskinesia (DYSK) units, and those with no significant correlation (R^2<0.4) to either behavior were classified as on-unclassified (ON) units (Figures 3A-3F). Putative dMSNs with firing rates correlated to both dyskinesia and rotation rate were labeled MIXED (Figure 3E).

To determine the timing of firing rate change relative to dyskinesia, firing rates of putative dMSN subpopulations (ON, ROT, DYSK) were averaged in 2 second bins and aligned to the start and end of visible dyskinesia (Figures 3I and Figures S4B-S4C). The onset of levodopa-evoked firing rate change was calculated as the *first* of two consecutive bins in which the firing rate exceeded the 99% confidence interval of the pre-dyskinesia baseline period. The offset of levodopa-evoked firing rate change was calculated as the *last* of two consecutive bins in which the firing rate exceeded the 99% confidence interval of post-dyskinesia baseline period. The pre-dyskinesia baseline was defined using the firing rate 150-200 seconds prior to the onset of dyskinesia. The post-dyskinesia baseline was defined using the firing rate 150-200 seconds following the end of dyskinesia. We then calculated the time difference between onset/offset of levodopa-evoked firing rate change and the start/end of dyskinesia to identify the latency and proportion of units whose firing rate change preceded the change in dyskinesia.

Using defined locomotor and grooming epochs (see the Behavior section above), we calculated the average firing rate of putative dMSNs during immobile and mobile bouts (Figures S1L-S1N, top), as well as during grooming (Figure 4D). For a more continuous analysis of locomotion, we also correlated firing rate to instantaneous velocity (using 1 second bins) in increments of 1 cm/s. Given the differences in baseline firing rates between groups, we normalized the firing rates of all MSNs, dMSNs, and iMSNs (Figures S1L-S1N, bottom) to their respective group average firing rate for the 0-1 cm/s velocity bin.

Firing rates recorded in the ipsilesional striatum of parkinsonian mice before (Park) or after (LID) levodopa were compared to recordings from healthy mice (Ctrl, Figures 1G-1H and S1L-S1M) and the contralesional striatum of parkinsonian mice (Contra, Figures S1L-S1M) using Mann-Whitney tests. Firing rates of parkinsonian mice before (Park) and after drug administration (levodopa (LID), Figure 1G-1H; SKF-81297 (SKF) or Quinpirole (Quin), Figure S2E, S2J) were compared using Wilcoxon signed-rank test (denoted Wilcoxon). Comparisons of firing rates between putative dMSN subtypes (ON, ROT, DYSK) and MSNs in healthy controls were made using a One-Way ANOVA with Tukey post-hoc test (Figure 3H). For experiments involving two doses of levodopa, firing rates between parkinsonian, sub-dyskinetic dose, and dyskinetic dose conditions were compared using Wilcoxon tests (Figure 4C).

Optogenetic Stimulation—Comparisons of rotation rate and AIM score (Figures 2D-2F) between healthy and parkinsonian mice (LD-naive or LD-treated) were conducted using a Mann-Whitney test. Comparisons within parkinsonian mice (between LD-naive and LD-treated conditions) were conducted using a Wilcoxon test.

Supplementary Material

Refer to Web version on PubMed Central for supplementary material.

Acknowledgements

The authors wish to thank Drs. Dorit Ron, Evan Feinberg, Massimo Scanziani, and members of the Nelson lab for valuable discussion, in particular Jonathan Schor for additional assistance with supplemental videos. This work was supported by grants from the NINDS (K08 NS081001) and Parkinson's Disease Foundation (PDF-JFA-1688), and the Richard and Shirley Cahill Endowed Chair in Parkinson's Disease Research (ABN).

References

Ahlskog JE, and Muenter MD (2001). Frequency of levodopa-related dyskinesias and motor fluctuations as estimated from the cumulative literature. Mov. Disord. Off. J. Mov. Disord. Soc 16, 448–458.

Albin RL, Young AB, and Penney JB (1989). The functional anatomy of basal ganglia disorders. Trends Neurosci 12, 366–375. [PubMed: 2479133]

Alcacer C, Andreoli L, Sebastianutto I, Jakobsson J, Fieblinger T, and Cenci MA (2017). Chemogenetic stimulation of striatal projection neurons modulates responses to Parkinson's disease therapy. J. Clin. Invest 127, 720–734. [PubMed: 28112685]

Barbera G, Liang B, Zhang L, Gerfen CR, Culurciello E, Chen R, Li Y, and Lin D-T (2016). Spatially Compact Neural Clusters in the Dorsal Striatum Encode Locomotion Relevant Information. Neuron 92, 202–213. [PubMed: 27667003]

Bergman H, Wichmann T, Karmon B, and DeLong MR (1994). The primate subthalamic nucleus. II. Neuronal activity in the MPTP model of parkinsonism. J. Neurophysiol 72, 507–520. [PubMed: 7983515]

Berke JD, Okatan M, Skurski J, and Eichenbaum HB (2004). Oscillatory entrainment of striatal neurons in freely moving rats. Neuron 43, 883–896. [PubMed: 15363398]

Boraud T, Bezard E, Guehl D, Bioulac B, and Gross C (1998). Effects of L-DOPA on neuronal activity of the globus pallidus externalis (GPe) and globus pallidus internalis (GPi) in the MPTP-treated monkey. Brain Res 787, 157–160. [PubMed: 9518590]

Carta M, Lindgren HS, Lundblad M, Stancampiano R, Fadda F, and Cenci MA (2006). Role of striatal L-DOPA in the production of dyskinesia in 6-hydroxydopamine lesioned rats. J. Neurochem 96, 1718–1727. [PubMed: 16539687]

Cenci MA, and Lundblad M (2007). Ratings of L-DOPA-induced dyskinesia in the unilateral 6-OHDA lesion model of Parkinson's disease in rats and mice. Curr. Protoc. Neurosci Editor. Board Jacqueline N Crawley Al *Chapter 9*, Unit 9.25.

Chen M-T, Morales M, Woodward DJ, Hoffer BJ, and Janak PH (2001). In Vivo Extracellular Recording of Striatal Neurons in the Awake Rat Following Unilateral 6-Hydroxydopamine Lesions. Exp. Neurol 171, 72–83. [PubMed: 11520122]

Costa RM, Lin S-C, Sotnikova TD, Cyr M, Gainetdinov RR, Caron MG, and Nicolelis MAL (2006). Rapid alterations in corticostriatal ensemble coordination during acute dopamine-dependent motor dysfunction. Neuron 52, 359–369. [PubMed: 17046697]

Cui G, Jun SB, Jin X, Pham MD, Vogel SS, Lovinger DM, and Costa RM (2013). Concurrent activation of striatal direct and indirect pathways during action initiation. Nature 494, 238–242. [PubMed: 23354054]

Deffains M, Iskhakova L, Katabi S, Haber SN, Israel Z, and Bergman H (2016). Subthalamic, not striatal, activity correlates with basal ganglia downstream activity in normal and parkinsonian monkeys. ELife 5.

DeLong MR (1990). Primate models of movement disorders of basal ganglia origin. Trends Neurosci 13, 281–285. [PubMed: 1695404]

Fieblinger T, Graves SM, Sebel LE, Alcacer C, Plotkin JL, Gertler TS, Chan CS, Heiman M, Greengard P, Cenci MA, et al. (2014). Cell type-specific plasticity of striatal projection neurons in parkinsonism and L-DOPA-induced dyskinesia. Nat. Commun 5, 5316. [PubMed: 25360704]

Filion M, and Tremblay L (1991). Abnormal spontaneous activity of globus pallidus neurons in monkeys with MPTP-induced parkinsonism. Brain Res 547, 142–151. [PubMed: 1677607]

Francardo V, Recchia A, Popovic N, Andersson D, Nissbrandt H, and Cenci MA (2011). Impact of the lesion procedure on the profiles of motor impairment and molecular responsiveness to L-DOPA in the 6-hydroxydopamine mouse model of Parkinson's disease. Neurobiol. Dis 42, 327–340. [PubMed: 21310234]

Gage GJ, Stoetzner CR, Wiltschko AB, and Berke JD (2010). Selective activation of striatal fast-spiking interneurons during choice execution. Neuron 67, 466–479. [PubMed: 20696383]

Galvan A, Devergnas A, and Wichmann T (2015). Alterations in neuronal activity in basal ganglia-thalamocortical circuits in the parkinsonian state. Front. Neuroanat 9, 5. [PubMed: 25698937]

Gerfen CR, and Surmeier DJ (2011). Modulation of striatal projection systems by dopamine. Annu. Rev. Neurosci 34, 441–466. [PubMed: 21469956]

Gerfen CR, Engber TM, Mahan LC, Susel Z, Chase TN, Monsma FJ, and Sibley DR (1990). D1 and D2 dopamine receptor-regulated gene expression of striatonigral and striatopallidal neurons. Science 250, 1429–1432. [PubMed: 2147780]

Gerfen CR, Paletzki R, and Heintz N (2013). GENSAT BAC cre-recombinase driver lines to study the functional organization of cerebral cortical and basal ganglia circuits. Neuron 80, 1368–1383. [PubMed: 24360541]

Gong S, Doughty M, Harbaugh CR, Cummins A, Hatten ME, Heintz N, and Gerfen CR (2007). Targeting Cre Recombinase to Specific Neuron Populations with Bacterial Artificial Chromosome Constructs. J. Neurosci 27, 9817–9823. [PubMed: 17855595]

Haber SN, Fudge JL, and McFarland NR (2000). Striatonigrostriatal pathways in primates form an ascending spiral from the shell to the dorsolateral striatum. J. Neurosci. Off. J. Soc. Neurosci 20, 2369–2382.

Harris KD, Henze DA, Csicsvari J, Hirase H, and Buzsáki G (2000). Accuracy of tetrode spike separation as determined by simultaneous intracellular and extracellular measurements. J. Neurophysiol 84, 401–414. [PubMed: 10899214]

Heiman M, Heilbut A, Francardo V, Kulicke R, Fenster RJ, Kolaczyk ED, Mesirov JP, Surmeier DJ, Cenci MA, and Greengard P (2014). Molecular adaptations of striatal spiny projection neurons during levodopa-induced dyskinesia. Proc. Natl. Acad. Sci. U. S. A 111, 4578–4583. [PubMed: 24599591]

Hernández-López S, Bargas J, Surmeier DJ, Reyes A, and Galarraga E (1997). D1 receptor activation enhances evoked discharge in neostriatal medium spiny neurons by modulating an L-type Ca2+ conductance. J. Neurosci. Off. J. Soc. Neurosci 17, 3334–3342.

Hernández-López S, Tkatch T, Perez-Garci E, Galarraga E, Bargas J, Hamm H, and Surmeier DJ (2000). D2 dopamine receptors in striatal medium spiny neurons reduce L-type Ca2+ currents and excitability via a novel PLC[beta]1-IP3-calcineurin-signaling cascade. J. Neurosci. Off. J. Soc. Neurosci 20, 8987–8995.

Horstink MW, Zijlmans JC, Pasman JW, Berger HJ, and van't Hof MA (1990). Severity of Parkinson's disease is a risk factor for peak-dose dyskinesia. J. Neurol. Neurosurg. Psychiatry 53, 224–226. [PubMed: 2324754]

Jenner P (2008). Molecular mechanisms of L-DOPA-induced dyskinesia. Nat. Rev. Neurosci 9, 665–677. [PubMed: 18714325]

Jin X, Tecuapetla F, and Costa RM (2014). Basal ganglia subcircuits distinctively encode the parsing and concatenation of action sequences. Nat. Neurosci 17, 423–430. [PubMed: 24464039]

Ketzef M, Spigolon G, Johansson Y, Bonito-Oliva A, Fisone G, and Silberberg G (2017). Dopamine Depletion Impairs Bilateral Sensory Processing in the Striatum in a Pathway-Dependent Manner. Neuron 94, 855–865.e5. [PubMed: 28521136]

Kish LJ, Palmer MR, and Gerhardt GA (1999). Multiple single-unit recordings in the striatum of freely moving animals: effects of apomorphine and d-amphetamine in normal and unilateral 6-hydroxydopamine-lesioned rats. Brain Res 833, 58–70. [PubMed: 10375677]

Kravitz AV, Freeze BS, Parker PRL, Kay K, Thwin MT, Deisseroth K, and Kreitzer AC (2010). Regulation of parkinsonian motor behaviours by optogenetic control of basal ganglia circuitry. Nature 466, 622–626. [PubMed: 20613723]

Kravitz AV, Owen SF, and Kreitzer AC (2013). Optogenetic identification of striatal projection neuron subtypes during in vivo recordings. Brain Res 1511, 21–32. [PubMed: 23178332]

Levy R, Dostrovsky JO, Lang AE, Sime E, Hutchison WD, and Lozano AM (2001). Effects of apomorphine on subthalamic nucleus and globus pallidus internus neurons in patients with Parkinson's disease. J. Neurophysiol 86, 249–260. [PubMed: 11431506]

Liang L, DeLong MR, and Papa SM (2008). Inversion of dopamine responses in striatal medium spiny neurons and involuntary movements. J. Neurosci. Off. J. Soc. Neurosci 28, 7537–7547.

Lozano AM, Lang AE, Levy R, Hutchison W, and Dostrovsky J (2000). Neuronal recordings in Parkinson's disease patients with dyskinesias induced by apomorphine. Ann. Neurol 47, S141–146. [PubMed: 10762141]

Mallet N, Ballion B, Le Moine C, and Gonon F (2006). Cortical inputs and GABA interneurons imbalance projection neurons in the striatum of parkinsonian rats. J. Neurosci. Off. J. Soc. Neurosci 26, 3875–3884.

McGeorge AJ, and Faull RL (1987). The organization and collateralization of corticostriate neurones in the motor and sensory cortex of the rat brain. Brain Res 423, 318–324. [PubMed: 2445449]

Oye C, Bouchard R, Boucher R, and Poirier LJ (1970). Spontaneous activity of the putamen after chronic interruption of the dopaminergic pathway: effect of L-dopa. J. Pharmacol. Exp. Ther 175, 700–708. [PubMed: 5489925]

Papa SM, Desimone R, Fiorani M, and Oldfield EH (1999). Internal globus pallidus discharge is nearly suppressed during levodopa-induced dyskinesias. Ann. Neurol 46, 732–738. [PubMed: 10553990]

Perez XA, Zhang D, Bordia T, and Quik M (2017). Striatal D1 medium spiny neuron activation induces dyskinesias in parkinsonian mice. Mov. Disord. Off. J. Mov. Disord. Soc

Picconi B, Centonze D, Håkansson K, Bernardi G, Greengard P, Fisone G, Cenci MA, and Calabresi P (2003). Loss of bidirectional striatal synaptic plasticity in L-DOPA-induced dyskinesia. Nat. Neurosci 6, 501–506. [PubMed: 12665799]

Planert H, Berger TK, and Silberberg G (2013). Membrane properties of striatal direct and indirect pathway neurons in mouse and rat slices and their modulation by dopamine. PloS One 8, e57054. [PubMed: 23469183]

Redgrave P, Rodriguez M, Smith Y, Rodriguez-Oroz MC, Lehericy S, Bergman H, Agid Y, DeLong MR, and Obeso JA (2010). Goal-directed and habitual control in the basal ganglia: implications for Parkinson's disease. Nat. Rev. Neurosci 11, 760–772. [PubMed: 20944662]

Rothwell PE, Hayton SJ, Sun GL, Fuccillo MV, Lim BK, and Malenka RC (2015). Input- and Output-Specific Regulation of Serial Order Performance by Corticostriatal Circuits. Neuron 88, 345–356. [PubMed: 26494279]

Shen W, Plotkin JL, Francardo V, Ko WKD, Xie Z, Li Q, Fieblinger T, Wess J, Neubig RR, Lindsley CW, et al. (2015). M4 Muscarinic Receptor Signaling Ameliorates Striatal Plasticity Deficits in Models of L-DOPA-Induced Dyskinesia. Neuron 88, 762–773. [PubMed: 26590347]

Soares J, Kliem MA, Betarbet R, Greenamyre JT, Yamamoto B, and Wichmann T (2004). Role of external pallidal segment in primate parkinsonism: comparison of the effects of 1-methyl-4-phenyl-1,2,3,6-tetrahydropyridine-induced parkinsonism and lesions of the external pallidal segment. J. Neurosci. Off. J. Soc. Neurosci 24, 6417–6426.

Yoshida M (1991). The neuronal mechanism underlying parkinsonism and dyskinesia: differential roles of the putamen and caudate nucleus. Neurosci. Res 12, 31–40. [PubMed: 1660992]

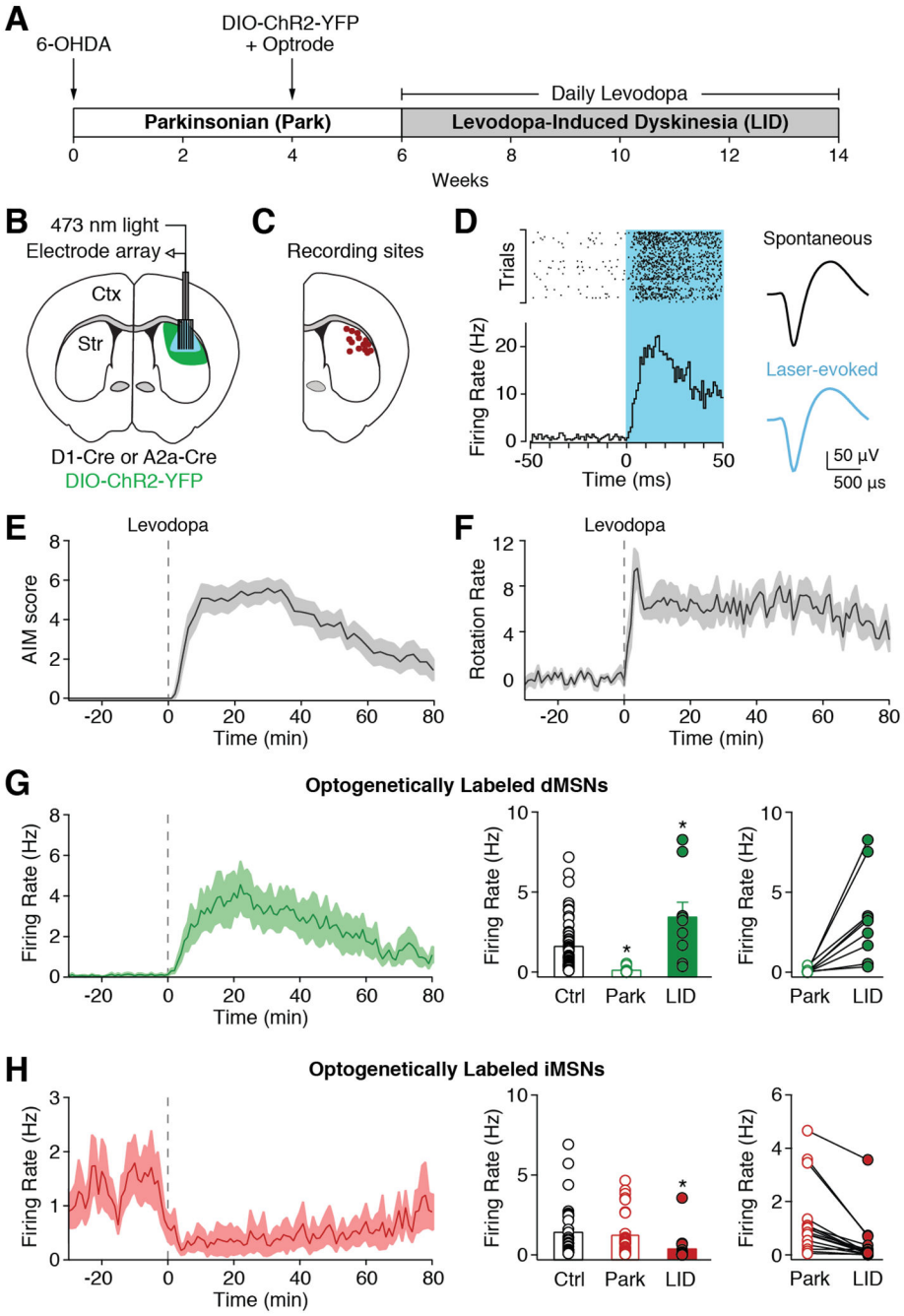

Figure 1. Alterations in Identified Striatal Neurons Following Dopamine Depletion and Replacement with Levodopa.

(A) Experimental timeline. **(B)** Schematic of optrode in dorsolateral striatum (DLS). **(C)** Recording sites verified by electrolytic lesions. **(D)** Example of optogenetically labeled striatal direct pathway neuron (dMSN). Left: PSTH and peri-event raster aligned to laser onset. Right: average spontaneous and laser-evoked waveforms. **(E-H)** Levodopa was administered at t=0 (dotted line). **(E)** Average dyskinesia, as measured by the Abnormal Involuntary Movement (AIM) score (N=12). **(F)** Average rotations (contralesional-

ipsilesional) per minute (N=12). **(G)** Left: average firing rate of optogenetically labeled dMSNs. Middle: dMSN firing rates in healthy mice (Ctrl, n=64, N=5) and parkinsonian mice before (Park, n=14, N=10) and after (LID, n=9, N=6) levodopa injection. Right: firing rate of individual dMSNs before and after levodopa. **(H)** Left: average firing rate of optogenetically labeled striatal indirect pathway neurons (iMSNs). Middle: iMSN firing rates in healthy mice (Ctrl, n=34, N=5) and parkinsonian mice before (Park, n=32, N=8) and after (LID, n=16, N=6) levodopa injection. Right: firing rate of individual iMSNs before and after levodopa. n=cells, N=animals. *$p<0.05$ vs Ctrl. All data presented as mean ± SEM. See also Figures S1 and S2.

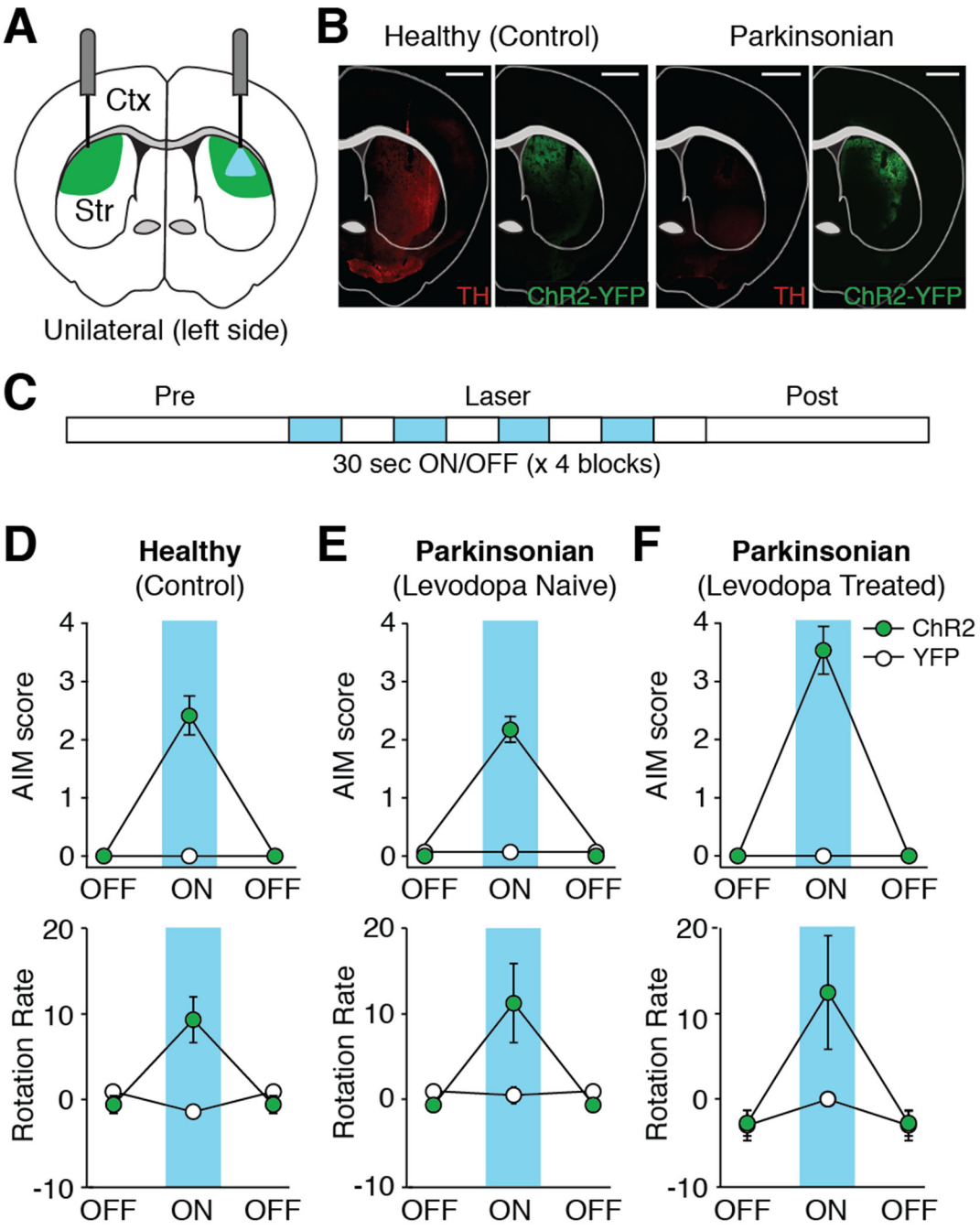

Figure 2. Optogenetic Activation of dMSNs Produces Dyskinesia in Healthy and Parkinsonian Mice.

(A) Schematic showing optic fiber placement and laser stimulation in the left (ipsilesional) DLS of parkinsonian mice. Green = DIO-ChR2-YFP expression. **(B)** Representative coronal sections from healthy and parkinsonian D1-Cre mice showing tyrosine hydroxylase (TH) staining and DIO-ChR2-YFP expression. Scale bar = 1mm. **(C)** Experimental timeline. **(D-F)** Behavior before (OFF) and during (ON) dMSN stimulation. Top: average dyskinesia (AIM) score. Bottom: average rotation rate. **(D)** Healthy mice (ChR2: N=12, YFP: N=11).

(E-F) Parkinsonian mice (ChR2: N=8, YFP: N=4) **(E)** before levodopa exposure and **(F)** after 2 weeks of chronic levodopa. N=animals. All data presented as mean ± SEM. See also Figure S3 and Movie S1.

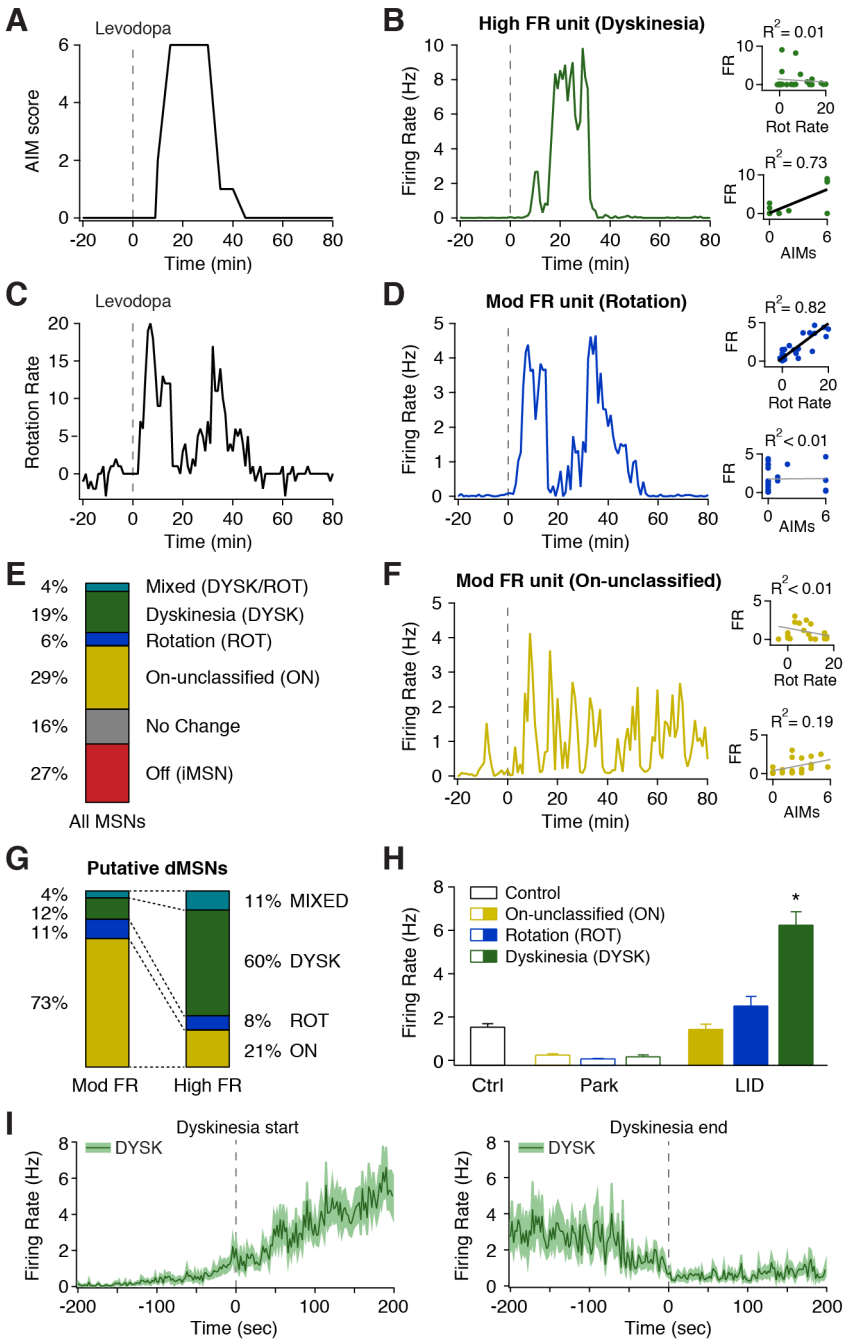

Figure 3. A Subpopulation of dMSNs Show High Firing Rates Correlated to Dyskinesia.

(A-D) Behavior and single unit firing rates from a representative session. **(A)** Dyskinesia score. **(B)** Representative putative dMSN classified as High FR whose firing rate was correlated with dyskinesia score (DYSK). **(C)** Rotation rate. **(D)** Representative putative dMSN classified as Mod FR whose firing rate was correlated with rotation rate (ROT). **(E)** Fraction of all putative MSNs (n=255, N=15) classified by behavioral correlation. **(F)** Representative putative dMSN classified as Norm FR whose firing rate was uncorrelated with rotation rate or AIM score (ON). **(B,D,F)** Insets: correlation between firing rate and

rotation rate (top) and dyskinesia (bottom). **(G)** Fraction of putative dMSNs classified by rate and their correlation to behavior (n=146, N=15). **(H)** Average firing rate of putative dMSNs based on correlation to behavior, before (Park) and after (LID) levodopa injection, compared to MSNs from healthy (Ctrl) mice. Ctrl: n=98, N=10; ON: n=74, ROT: n=14, DYSK: n=47, N=15. *p<0.05 vs Ctrl. **(I)** Average firing rate of DYSK units aligned to dyskinesia start (left, n=43) and end (right, n=37, N=15). n=cells, N=animals. All data presented as mean ± SEM. See also Figure S4 and Movie S2.

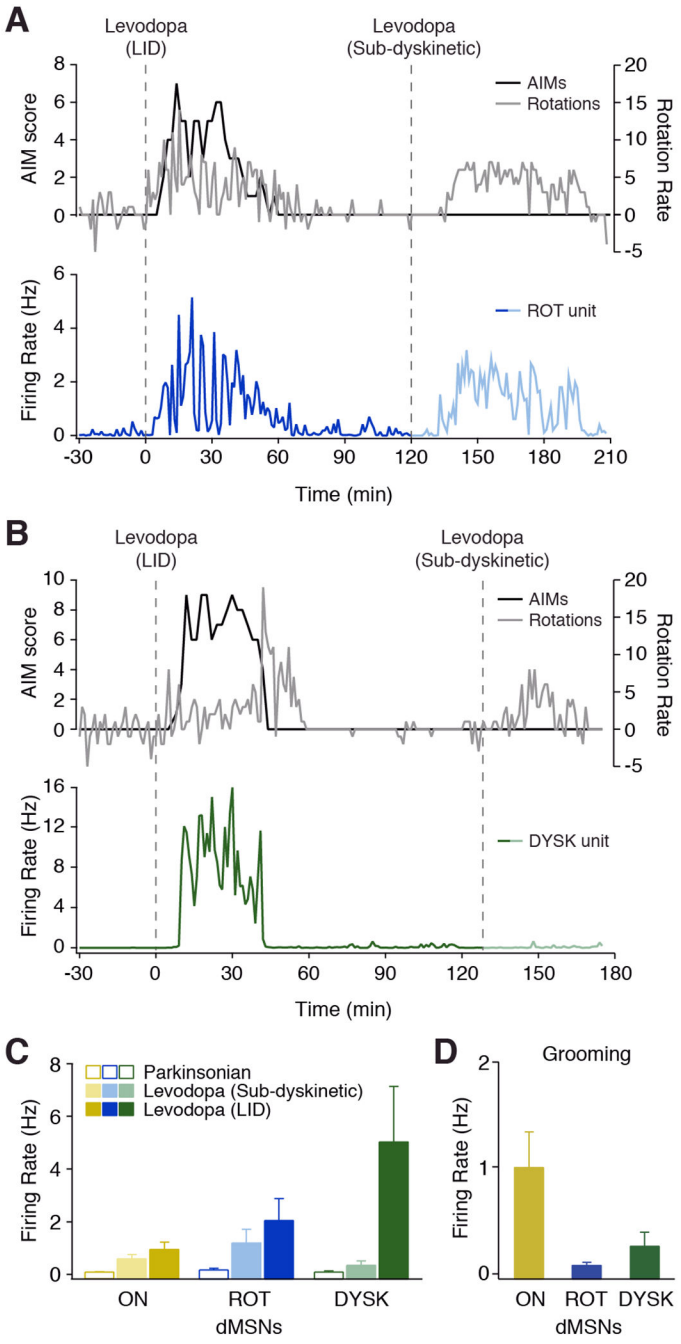

Figure 4. DYSK Unit Activity is Specific to LID

(A-B) Two doses of levodopa were administered in a single session. Top: dyskinesia score (black) and rotation rate (gray). Bottom: unit firing rate, aligned to levodopa injection (dotted line). Representative **(A)** ROT unit and **(B)** DYSK unit**. (C)** Average firing rate of putative dMSN subtypes before (parkinsonian) and after dyskinetic and sub-dyskinetic doses of levodopa. ON: n=14, N=4; ROT: n=8, N=3; DYSK: n=8, N=3. **(D)** Average firing rate of

putative dMSN subtypes during grooming (ON: n=30, N=4; ROT: n=5, N=2; DYSK: n=44, N=5). n=cells, N=animals. All data presented as mean ± SEM. See also Movie S3 and S4.